Abnormal Inversion Splitting in NH_2D: Rotational Analysis of the ν_5 Bending Vibrational Band System

Marjo Halonen* and Lauri Halonen

Laboratory of Physical Chemistry, P.O. Box 55 (A.I. Virtasen aukio 1), FIN-00014 University of Helsinki, Finland

Received: March 1, 2006; In Final Form: April 24, 2006

A high-resolution Fourier transform infrared spectrum of the ν_5 bending vibrational band system region of the partially deuterated ammonia molecule NH_2D has been measured and rotationally analyzed. The spectrum consists of strong a-type transitions between the states of same vibrational symmetry and weaker c-type transitions between the states of different vibrational symmetry. The Hamiltonian model used includes interaction terms between the rotational states of both upper and lower inversion doublets. The vibrational term values for the symmetric and the antisymmetric component of the upper-inversion doublet are 1605.637 965(620) cm^{-1} and 1590.993 82(100) cm^{-1}, respectively, where the numbers in parentheses are one-standard deviations in the least significant digit. These figures are close to the corresponding values 1605.62 cm^{-1} and 1590.72 cm^{-1} obtained recently from results based on high-level ab initio calculations. The order of the vibrational term values is abnormal in the ammonia family, as typically the symmetric state is lower in wavenumber than the antisymmetric one.

1. Introduction

The ammonia molecule NH_3 is characterized by a large amplitude inversion motion where nuclear tunneling occurs through the symmetrical planar configuration. The inversion barrier height is only about 1787 cm^{-1} in normal ammonia[1] and consequently the inversion motion gives rise to vibrational energy level splittings, the sizes of which depend on the vibrational state in question. For example, the inversion splittings are 0.79, 35.69, 1.03, 0.31, and 1.099 cm^{-1} for the ground, symmetrical bending (ν_2), symmetrical stretching (ν_1), antisymmetrical stretching (ν_3), and antisymmetrical bending (ν_4) states, respectively.[2−5] Usually, the symmetrical state with respect to reflection through a plane containing the planar transition state configuration is lower in energy than the antisymmetrical state. The vibration−rotation spectra are complicated due to these splittings because there are strong resonance interactions between the rotational states of the close-lying inversion states.

Ammonia provides an excellent test case for the quality of electronic structure calculation methods. It is possible to apply high-level theory because there are only 10 electrons in ammonia. The barrier height of the large amplitude inversion motion and consequently the experimentally observable inversion splittings are particularly sensitive to the fine details of the electronic structure. Indeed, there have been several computational studies in the past.[1,6−10] The most advanced one includes a high-order coupled cluster approach up to the pentuble level with the explicitly correlated R12 method, which contains an interelectronic distance in the wave function.[1] Diagonal corrections due to the failure of the Born−Oppenheimer approximation and corrections due to relativistic effects have also been included. Using this most advanced approach, it is possible to compute potential energy surface points with accuracy which allows the calculation of vibrational term values within 1 cm^{-1} and the inversion splitting within 0.1 cm^{-1} when compared with high-resolution experimental observations. The experimental uncertainty has not yet been reached, but the precision of the theoretical values is such that these methods provide accurate predictions of spectroscopic properties of small molecules. This is particularly pleasing for experimentally difficult species such as the hydronium ion H_3O^+ and its isotopic species.[10]

Deuterium containing molecules are useful probes when investigating conditions in interstellar and protostellar regions and early stages of star formation. NH_2D has been observed spectroscopically in dark molecular clouds and in protostellar cores, as well.[11,12] In this light, it is odd that the literature concerning high-precision spectroscopic measurements of the partly deuterated ammonia species NH_2D[13−18] and NHD_2[14,17−20] is sparse. Despite microwave, submillimeter, millimeter, and far-infrared measurements, the only NH_2D infrared band system studied using high-resolution techniques is the symmetric bending mode ν_2 (A_1/B_1) with the upper vibrational states at 876.37 cm^{-1} and 896.56 cm^{-1}, for the symmetric and the antisymmetric component, respectively.[14−16] In addition, the electronic transition $\tilde{A} \leftarrow \tilde{X}$ centered above 46 000 cm^{-1} has also been studied.[21] There is room for more work in this area.

This article concentrates on the ν_5 (A_1/B_1) bending vibrational band system of NH_2D, where according to high-level ab initio calculations the inversion splitting is reversed in the upper state.[6,7] This is abnormal in behavior within the ammonia family, as typically the symmetric inversion state is lower in wavenumber than the antisymmetric one. It has been suggested that possibly a Fermi-resonance type anharmonic interaction of ν_5 with the first overtone of the symmetric bend, $2\nu_2$, is responsible for this anomaly.[7,22] The calculated positions of $2\nu_2^s$ and $2\nu_2^a$ are 1510.74 and 1736.68 cm^{-1}, respectively.[6] Thus, it is feasible that the symmetric states of ν_5 and $2\nu_2$, that is, ν_5^s and $2\nu_2^s$, interact, and as a result ν_5^s is pushed above the antisymmetric

10.1021/jp061287a CCC: $33.50

component ν_5^a, whereas the interaction of the antisymmetric component ν_5^a with $2\nu_2^a$ pushes ν_5^a down. The net result is that ν_5^s and ν_5^a are about 15 cm^{-1} apart, and the corresponding calculated vibrational term values are 1605.62 and 1590.72 cm^{-1}.[6]

In this contribution, we describe a high-resolution measurement of the ν_5 (A_1/B_1) bending vibrational band system of NH_2D and its rotational analysis. This analysis is somewhat demanding because there is a strong vibration−rotation coupling between the rotational states of both upper (ν_5^s and ν_5^a) and lower (ν_0^s and ν_0^a) inversion states. Thus, a standard isolated asymmetric band model does not work and it is necessary to include vibration−rotation interaction terms in the effective Hamiltonian model. An important aim of this study is to find out how well potential energy surfaces based on state-of-the-art ab initio calculations can be used to predict the experimental band centers in such a vibrationally perturbed system as ν_5.

The organization of the paper is such that, in section 2, experimental details including the time dependence of the degree of deuteration in the sample cell are discussed, section 3 deals with the vibration−rotation model and the rotational fine structure analysis, section 4 gives the results, and section 5 concludes with a discussion.

2. Experimental Method

A multipass cell was initially filled with 10 mbars of ND_3 (99 at. % D, Isotec Inc.), and an optical path length of 7.68 m was chosen. The cell placed inside the sample compartment of the infrared spectrometer and the connecting vacuum line were pumped with a diffusion pump prior to introducing the sample to the cell. This was done thoroughly to minimize the amount of residual water. We used the Bruker 120 IFS high-resolution FTIR spectrometer equipped with a globar source, a KBr beam splitter, and an MCT detector. An optical band-pass filter of the wavenumber range 1000−2000 cm^{-1} was employed. The number of coadded scans varied typically from 60 to 65. A weak Norton−Beer apodization and a Mertz phase correction mode were used. The observed line width (fwhm) is around 0.007 cm^{-1}, although somewhat lower resolution spectra were also taken for comparison. Residual water vapor peaks were employed for the spectral calibration.[23] The line position accuracy with respect to the published calibration lines was estimated to be better than 0.0005 cm^{-1}.

Some overview spectra in the region 1000−4000 cm^{-1} were recorded in addition to the high-resolution spectra of the ν_5 band system of NH_2D. Several bands of ND_3 are observed in these spectra. Fortunately, the wavenumber region of the ν_5 (A_1/B_1) band of NH_2D is relatively free from interfering ND_3 peaks, because in ND_3 the symmetric component of the second overtone of ν_2, $3\nu_2^s$ (A_1'), around 1825 cm^{-1} is weak and does not extend far from the band center, and the antisymmetric component of the combination band $\nu_2 + \nu_4^a$ (E'') calculated to be around 1635 cm^{-1} could not be observed.[13] The antisymmetric component of the first overtone of the ν_2 band, $2\nu_2^a$ (A_1''), of ND_3 located around 1429 cm^{-1} is also weak and is buried under the much stronger ν_6 (B_2/A_2) fundamental of NHD_2 centered at 1462 cm^{-1}.

ND_3 started to exchange deuterium atoms with hydrogen atoms of the residual water after having been introduced to the cell, even though the sample cell and the vacuum line had been pumped thoroughly. The NH_2D peaks were soon apparent in the spectrum. Thus, it was unnecessary to mix ND_3 with NH_3 to obtain the NH_2D spectrum. We were also able to monitor the evolution of the spectrum as a function of time. After we added ND_3 to the multipass cell, the sample was left in the cell for over 1 week, and spectra were recorded regularly to obtain the most optimal spectrum of NH_2D. The ν_6 (B_2/A_2) band of NHD_2 centered at 1462 cm^{-1} was immediately observable and was very strong, whereas the intensity of the ν_5 (A_1/B_1) band of NH_2D increased day by day. Finally, it became so strong that in the last spectra taken about 1 week after the addition of the sample, the optical path length of the multipass cell had to be reduced to one-half of the original value (3.84 m vs 7.68 m) and the pressure of the sample had to be decreased to one-third by pumping. The Q branch region ($\Delta J = J' - J'' = 0$, where the total angular momentum quantum numbers J' and J'' refer

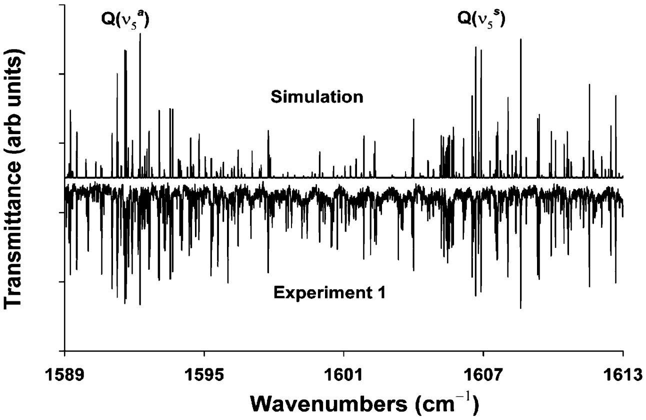

Figure 1. Q branch region of the symmetric (ν_5^s) and the antisymmetric (ν_5^a) components of the ν_5 (A_1/B_1) bending vibrational band system of NH_2D. The simulated spectrum is above and a spectrum measured immediately after adding the ND_3 sample to the cell (experiment 1) is below. The Q branch of the ν_5 band of NH_2D partly coincides with the P branch of the ν_6 (B_2/A_2) band of NHD_2, which explains the additional strong peaks in the experimental spectrum.

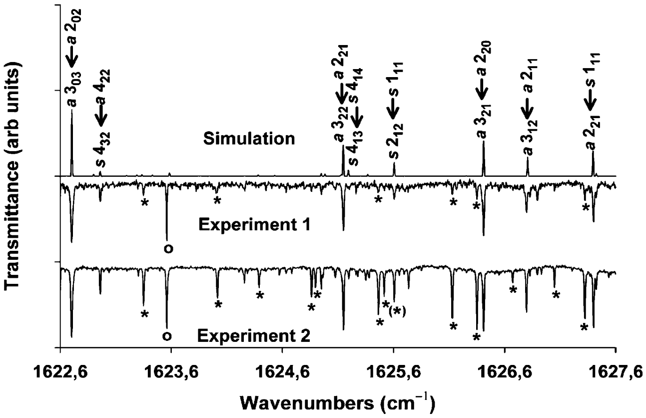

Figure 2. Part of the ν_5 (A_1/B_1) band of NH_2D expanded. The first spectrum (experiment 1) was measured immediately after adding the ND_3 sample to the cell and the second one (experiment 2) about 1 week later. The simulated spectrum is above. The strongest transitions are marked using the notation $\Gamma' J'_{K_a'K_c'} \leftarrow \Gamma'' J''_{K_a''K_c''}$, where Γ is the symmetry of the state (s refers to the symmetric and a to the antisymmetric state), J is the total angular momentum quantum number, and K_a and K_c are the near prolate and oblate symmetric top K quantum numbers, respectively. The single prime refers to the upper state and the double prime to the lower state. The NH_3 peaks are marked with the symbol *, and their positions have been taken from refs 5 and 24. The symbol (*) is used for a transition that overlaps with a peak of NH_3. The symbol "o" refers to a peak of H_2O. As the amount of NH_2D grew day by day, the optical path length of the second spectrum was reduced to one-half and the pressure of the sample to one-third of that of the first spectrum. The number of scans added together is 60 and 65 in experiments 1 and 2, respectively.

to the upper and lower states, respectively) of the ν_5 (A_1/B_1) band system of NH_2D is shown in Figure 1. The spectrum extends about from 1480 to 1740 cm^{-1}. The first overtone of ν_2, $2\nu_2$ (A_1/B_1), which would according to the calculations have band centers at 1510.74 and 1736.68 cm^{-1}, is too weak to affect the rotational analysis of ν_5.

The NHD_2 peaks become weaker with respect to the NH_2D peaks in the last spectra taken. In addition, in NH_3, the ν_4 (E) band with band centers at 1626.276 and 1627.375 cm^{-1} for the symmetric and the antisymmetric component,[5] respectively, is barely apparent in the first spectrum, whereas in the last spectra its strongest peaks are as intense as some of the strong NH_2D peaks. The amount of NH_3 is still low, as its peaks are mainly observed in the Q branch region of the ν_4 band. The antisymmetric component of the $2\nu_2$ (A_1) band of NH_3 centered at 1597.47 cm^{-1} [5] is so much weaker compared to the ν_4 band that only a few peaks are noticeable in the last spectra. The NH_3 peaks belonging to the bands ν_4 and $2\nu_2$ are easily recognizable as they have been reported in the literature.[5,24]

Part of the ν_5 band of NH_2D, measured directly after adding the sample to the cell and about 1 week afterward, are shown in Figure 2. In the first spectrum, the NH_2D peaks are weak, and in the last spectrum, they have grown substantially. The development of the Q branch of the ν_4 (E) band of NH_3 is also worth noticing.

3. Rotational Analysis

The vibrationally diagonal Hamiltonian for the symmetric and antisymmetric component of the ground state and of the ν_5 (A_1/B_1) upper state of NH_2D is[25]

$$H/hc = \nu + AJ_x^{\,2} + BJ_y^{\,2} + CJ_z^{\,2} - D_J J^4 - D_{JK} J^2 J_z^{\,2} - D_K J_z^{\,4} + H_J J^6 + H_{JK} J^4 J_z^{\,2} + H_{KJ} J^2 J_z^{\,4} + H_K J_z^{\,6} + L_J J^8 + L_{JJK} J^6 J_z^{\,2} + L_{JK} J^4 J_z^{\,4} + L_{KKJ} J^2 J_z^{\,6} + L_K J_z^{\,8} + (d_1 J^2 + h_1 J^4 + l_1 J^6)(J_+^{\,2} + J_-^{\,2}) + (d_2 + h_2 J^2 + l_2 J^4)(J_+^{\,4} + J_-^{\,4}) + (h_3 + l_3 J^2)(J_+^{\,6} + J_-^{\,6}) + l_4(J_+^{\,8} + J_-^{\,8})$$

where J_x, J_y, and J_z are the molecule-fixed Cartesian components of the total angular momentum operator $\mathbf{J}$, $J^2 = |\mathbf{J}|^2$, $J_\pm = J_x \mp iJ_y$, ν is the vibrational term value measured from the symmetrical ground vibrational state, A, B, and C are rotational constants, and D, H, and L are centrifugal distortion parameters. The Hamiltonian has the same form for all the four vibrational states in question, but every state has its own set of rotational parameters. The corresponding vibrational superscripts/subscripts have been omitted for the sake of clarity.

The rotational states of the close-lying inversion levels have been analyzed simultaneously. The appropriate Hamiltonian operator, which takes into account the interactions between the rotational states of the near degenerate symmetric and the antisymmetric vibrational states, is

$$H_{01}/hc = F(J_xJ_z + J_zJ_x) + F_J J^2(J_xJ_z + J_zJ_x) + F_K[J_z^{\,2}(J_xJ_z + J_zJ_x) + (J_xJ_z + J_zJ_x)J_z^{\,2}]$$

where the parameter F describes the strength of this interaction, and F_J and F_K give the $J(J + 1)$ and K^2 dependence of F, respectively. The quantum label J is the total angular momentum quantum number and the K quantum number corresponds to the angular momentum component along the molecule fixed C_3 axis (z axis). The interaction parameters F_J and F_K have not been determinable for the ground state.[17] In our analysis, the parameter F_K could not be determined with significance for the upper states, and therefore it was constrained to zero.

We used Watson's choice of phase.[25] This is mentioned because it affects the signs of the parameters d_1, h_1, h_3, l_1, and l_3.[15] The S reduction and representation III^r were adopted. We employed our own computer program written in Fortran especially for the analysis of the present spectrum. The program includes a part where the Hamiltonian parameters can be optimized with the nonlinear least-squares method using observed vibration−rotation transition wavenumbers as data. Infrared absorption spectrum including intensities for the vibration−rotation transitions can also be computed.

The R branch ($\Delta J = +1$) and slightly also the Q branch of the ν_5 band of NH_2D coincide with the P branch ($\Delta J = -1$) of the ν_6 (B_2/A_2) band of NHD_2. Thus, the P and Q branches of the ν_5 band, which are relatively free from interfering NHD_2 peaks, were used as starting points in analyzing the spectra. In addition, the Q branch region is free from water vapor peaks. Consequently, some recognizable rotational fine structure was readily observable, which helped in finding initial assignments. The ground state parameters were taken from ref 17 (set II).

To obtain an optimal signal-to-noise ratio for NH_2D, peak positions were taken from the spectrum measured about 1 week after adding the ND_3 sample to the cell. Altogether 350 transitions with up to $J' = 13$ were included in the final fit. Several peaks had to be left out due to perturbations, and the fit was found to be sensitive with respect to accidental inclusion of perturbed peaks. The perturbations will be discussed in the next section. In addition, peaks coinciding with those belonging to NH_3, NHD_2 or H_2O were omitted from the fit.

For the ground vibrational state, the nuclear spin weights are $g_{ee} = g_{eo} = 1$ and $g_{oo} = g_{oe} = 3$, where e refers to an even and o to an odd rotational state, i.e., even and odd in the asymmetric rotor K_a or K_c label (near prolate and oblate symmetric top K quantum numbers, respectively).[26] The first subscript in g refers to K_a and the second one to K_c. The a-type transitions, which occur between vibrational states of the same inversion symmetry (s ← s or a ← a), are by far the strongest ones and thus the spectrum is characterized by these transitions and correspondingly, due to the 15 cm^{-1} upper state inversion splitting, there are two strong central Q branches at about 1590 and 1605 cm^{-1} (see Figure 1). The weaker c-type transitions occur between vibrational states of different inversion symmetry (s ← a or a ← s). The relative vibrational transition dipole moments $\mu_{ss} = \mu_{aa} = 0.18$ D, $\mu_{sa} = 0.08$ D, and $\mu_{as} = 0.04$ D reproduced the intensities well, as can be seen from Figures 1−3. Other combinations of signs were also tried, but the above-mentioned choice was the best one, although the difference between the calculated spectra using different sign combinations was small in some other sign combinations. Interestingly, a comparison with the vibrational transition dipole moments of the inversion mode ν_2 shows that in ν_2 μ_{sa} and μ_{as} are much larger in magnitude than μ_{ss} and μ_{aa} whereas it is opposite in ν_5.[16]

4. Results and Discussion

The results of the upper state-fit of the ν_5 (A_1/B_1) band system of NH_2D are given in Table 1. Parts of the simulated spectrum calculated using the Hamiltonian parameters of Table 1 and the vibrational transition moments as given above can be seen in Figures 1−3.

The ν_5^s and ν_5^a band centers (or more precisely the vibrational term values measured from the symmetrical ground vibrational state) are 1605.637 965(620) and 1590.993 82(100) cm^{-1},

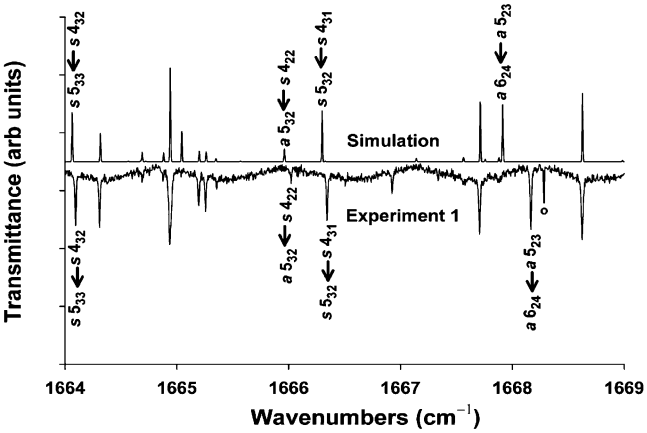

Figure 3. Some perturbed peaks of the ν_5 (A_1/B_1) band system of NH_2D are marked using the same notation as in Figure 2. The symbol "o" refers to a peak of H_2O.

respectively, where the numbers in parentheses are one-standard errors obtained from the nonlinear least-squares optimization of Hamiltonian parameters. They are pleasingly close to the corresponding values 1605.62 and 1590.72 cm^{-1} obtained from a variational calculation using a potential energy surface based on high-level ab initio calculations.[6] Another electronic structure calculation estimates the ν_5 band centers to be at 1607.26 and 1590.52 cm^{-1}, where especially the symmetric component is further away from the experimentally observed value.[7]

The interaction constant F for the upper states is well-defined ($F = -0.296\,792(130)$ cm^{-1}) and about twice as large in magnitude as in the ground state inversion doublet. As is seen from Table 1, we could also determine F_J for the upper states but F_K was constrained to zero. The rotational constants A, B, and C of the upper states are reasonably close to the corresponding ground state values, as expected. The largest change compared to the ground state is observed in the B constant. As we have mentioned before, the ν_5 bending vibrational band system of NH_2D is perturbed, and the centrifugal distortion parameters can often be anomalous in perturbed vibrational states. In the ν_5 band, the quartic centrifugal distortion constants are close to the corresponding ground state values, but many of the higher-order distortion constants deviate a lot from the corresponding ground state values.

Transitions whose upper states are clearly perturbed have not been included as data with nonzero weights in the least squares optimization of the Hamiltonian parameters. However, attaching zero weights to them helps in finding sequences of perturbed transitions and this procedure also reduces the risk in making misinterpretations. Thus, when there are two or more transitions that possess a common perturbed upper state, the differences between the observed and calculated transition wavenumbers are similar for all of them. This gives additional confirmation of the spectral interpretation. There are several perturbed peaks in the spectrum. The most obvious ones have been arranged according to their upper states in Table 2. One observes that there are several series of perturbed upper states with successive $J'_{K_a'K_c'}$ values. For instance, for $K_a' = 1$, the upper states 8_{18}, 9_{19}, and $10_{1\ 10}$ are perturbed in the symmetric component of the ν_5 band ($\nu_5{}^s$), whereas the states 7_{17} and $11_{1\ 11}$ are not and are thus included in the fit. The perturbation seems to be localized especially around $J' = 5-9$. Some of the perturbed peaks can be seen in Figure 3. Typically, the perturbations shift the peaks from their unperturbed positions by about 0.02–0.1 cm^{-1}, but the deviations can be even as large as 0.6 cm^{-1}.

It is clear that the perturbations are due to vibration–rotation interactions between the rotational states of ν_5 and $2\nu_2$. We adopted a simple procedure to find out more about these resonances. We calculated the upper state rotational energy levels of both the ν_5 and $2\nu_2$ bands of NH_2D using the computer program written for this paper. Estimates for the rotational constants of the $2\nu_2$ states were obtained using the formula $B_v = B_e - \alpha\,(v + {}^1/_2)$, where the vibrational quantum number $v = 0$, 1 or 2, and the α parameters describe the vibrational dependence of the rotational constants. The rotational constants of the ground and ν_2 states were taken from Table 1 and ref 16, respectively, and thus we were able to compute the A, B and C rotational constants for the $2\nu_2$ inversion doublet. The calculated values 1510.74 and 1736.68 cm^{-1} were employed for the vibrational term values of the symmetric and antisymmetric components of $2\nu_2$,[6] respectively, although a larger value 1525.78 cm^{-1} from ref 7 was also tested for the symmetric component. The interaction parameters F, F_J, and F_K of the $2\nu_2$ inversion doublet states were constrained to zero due to the large inversion splitting. The quartic centrifugal distortion constants of the $2\nu_2$ states were constrained to the values of the ν_2 states.[16]

The upper state rotational energy levels of ν_5 were calculated with the parameters of Table 1, and the corresponding $2\nu_2$ levels using the parameters obtained with the above-mentioned procedure. Our simple model indicates that there is indeed a possibility for Coriolis and α-type vibration–rotation resonances between the rotational states of ν_5 and $2\nu_2$.[27,28] Specifically, the rotational states $J'_{K_a'K_c'}$ of $\nu_5{}^s$ in Table 2 are probably perturbed by the nearby $2\nu_2{}^s$ $J'_{K_a'+2\ K_c'-2}$ states. On the other hand, the $\nu_5{}^a$ upper state rotational energy levels are too far from the corresponding $2\nu_2{}^a$ levels for resonances to occur, and some other interaction is responsible for the perturbations found in the antisymmetric state. It might be that most of the $\nu_5{}^a$ $J'_{K_a'K_c'}$ states in Table 2 are perturbed by the $2\nu_2{}^s$ $J'_{K_a'+1\ K_c'-1}$ states. These resonances are generally stronger than the ones found between the rotational states of the symmetric vibrational inversion states of ν_5 and $2\nu_2$. In addition, there might exist a high-order vibration–rotation resonance in the case of the $\nu_5{}^a$ 6_{24}, 7_{25} and 9_{27} states, which are almost coincidental in energy with the $2\nu_2{}^s$ $J'_{K_a'+3\ K_c'-3}$ states. However, one must bear in mind that the calculation of the $2\nu_2$ upper state rotational energy levels is approximate, even though it seems to give a reasonable explanation of the perturbations. A more thorough analysis would require to use of a more sophisticated model where the rotational states of ν_5 and $2\nu_2$ are explicitly coupled by the above-mentioned vibration–rotation interactions. However, this might be difficult to carry out in practice due to the weakness of the $2\nu_2$ band system.

There remain some peaks in the spectrum that do not belong to ND_3, ND_2H, NH_3, and H_2O nor to the ν_5 or the $2\nu_2$ bands of NH_2D. Most of them are not apparent in the spectrum taken immediately after adding the sample to the cell, but they can be large in the last spectra taken.

5. Summary and Conclusions

A high-resolution spectrum of the ν_5 bending vibrational band system of NH_2D has been measured and rotationally analyzed. A sample of ND_3 was left in a multipass cell, and the evolution of the spectrum from ND_3 to NHD_2, NH_2D and all the way to NH_3 was monitored. A rotational analysis of the ν_5 band system of NH_2D yielded band centers $\nu_5{}^s$ and $\nu_5{}^a$ that are close to those obtained by results based on the state-of-the-art ab initio calculations. Also, the reversed order of the inversion splitting, that is, the symmetric state is higher in wavenumber than the

TABLE 1: Results of the Upper State Fit of the ν_5 (A_1/B_1) Bending Vibrational Band System of NH_2D[a]

	GS^s	GS^a	$\nu_5{}^s$	$\nu_5{}^a$
ν	0	0.40592773307	1605.637965(620)	1590.99382(100)
A	9.677291775	9.674166274	9.762119(350)	9.681939(210)
B	6.4108862741	6.40974709545	6.586977(120)	6.562703(380)
C	4.696664828	4.697412045	4.694729(210)	4.718033(190)
$D_J/10^{-4}$	5.27440693	5.21275400	4.7062(240)	5.902(170)
$D_{JK}/10^{-4}$	−7.98473088	−7.85659554	−7.937(230)	−11.057(470)
$D_K/10^{-4}$	3.65232022	3.57977392	4.160(260)	6.703(340)
$d_1/10^{-4}$	−1.39353201	−1.36635075	−0.5541(270)	−0.7012(420)
$d_2/10^{-6}$	4.4675934	4.8613414	−4.25(130)	−53.33(140)
$H_J/10^{-7}$	1.2167885	1.0995211	1.2167885^b	22.98(370)
$H_{JK}/10^{-7}$	−2.8743139	−2.6216330	−197.03(600)	154.6(160)
$H_{KJ}/10^{-7}$	2.9717402	2.7230055	437.7(130)	−483.2(230)
$H_K/10^{-7}$	−1.2866940	−1.1703824	−241.96(810)	347.0(100)
$h_1/10^{-8}$	6.07762584	5.41259599	100.86(210)	−97.30(450)
$h_2/10^{-8}$	1.350145	1.1919487	−20.79(210)	11.20(230)
$h_3/10^{-9}$	1.1271592	1.2712347	−49.76(560)	235.61(920)
$L_J/10^{-11}$	−3.122131	−2.128930	−3.122131^b	−5637(230)
$L_{JJK}/10^{-11}$	9.3908927	6.6647575	6032(260)	76180(120)
$L_{JK}/10^{-10}$	−1.670972	−1.198571	−1.670972^b	−21536(230)
$L_{KJ}/10^{-10}$	1.691905	1.195026	−2300(120)	19803(200)
$L_K/10^{-11}$	−4.602900	−2.61760	17150(110)	−51875(760)
F	−0.1716059		−0.296792(130)	
$F_J/10^{-4}$	0		1.3438(430)	
$F_K/10^{-5}$	0		0^b	
$\delta_{fit}/10^{-3}$			2.9	

[a] Units are cm^{-1}. Uncertainties in parentheses represent one-standard deviation in the least significant digit. Uncertainties have been rounded to two digits. The symbol GS refers to the ground state. The ground state parameters have been taken from ref 17. The superscripts s and a refer to the symmetric and antisymmetric component of the state in question. The symbol δ_{fit} denotes for the standard deviation of the fit. [b] Constrained to the corresponding ground state value.

TABLE 2: Perturbed Upper States Found in the ν_5 Bending Vibrational Band System of NH_2D[a]

	$\nu_5{}^s$				$\nu_5{}^a$				
J'	$K_a' = 0$	$K_a' = 1$	$K_a' = 2$	$K_a' = 3$	$K_a' = 0$	$K_a' = 1$	$K_a' = 2$	$K_a' = 3$	$K_a' = 4$
4			4_{22}			4_{14}			
5			5_{24}	5_{32}, 5_{33}		5_{15}		5_{32}, 5_{33}	
6			6_{24}, 6_{25}	6_{33}, 6_{34}		6_{16}, 6_{15}	6_{24}, 6_{25}	6_{33}, 6_{34}	6_{43}
7			7_{26}	7_{34}, 7_{35}	7_{07}	7_{17}, 7_{16}	7_{25}	7_{35}	7_{43}, 7_{44}
8	8_{08}	8_{18}	8_{27}	8_{35}, 8_{36}	8_{08}	8_{18}	8_{27}	8_{36}	8_{44}, 8_{45}
9	9_{09}	9_{19}	9_{28}	9_{36}, 9_{37}	9_{09}	9_{19}	9_{27}, 9_{28}		9_{45}, 9_{46}
10	$10_{0\ 10}$	$10_{1\ 10}$			$10_{0\ 10}$	$10_{1\ 10}$			

[a] The superscript s is used for the symmetric component and a for the asymmetric component of the band.

antisymmetric one in the upper state, first found by high-level ab initio calculations, is confirmed. It is pleasing that modern electronic structure calculations and full variational calculations with exact kinetic energy operators for the nuclear motion are able to produce these results for a molecule containing a large amplitude inversion motion. It is clear that for NH_3-type molecules high-level electronic structure calculations are able to produce results that are accurate enough to help experimental work. The same kind of accuracy can be expected for an isoelectronic system H_3O^+ (H_2DO^+), and therefore computational methods can be used to accurately predict the positions of unknown bands for these experimentally demanding molecules.

A set of rotational parameters has been obtained for the upper states of the ν_5 band system. In addition, the interaction coefficients F and F_J, which couple the rotational states of the upper state inversion doublet, could be determined. Several series of perturbed peaks were found and a suggestion for possible perturbers was made. A comparison of the vibrational transition dipole moments of the current spectrum with those found for ν_2 shows an opposite type of behavior of ν_5: μ_{ss} and μ_{aa} are much larger than μ_{sa} and μ_{as}. The same relative signs for all the vibrational transition dipole moments were found to produce the experimental spectrum very well.

Our study involving high-quality vibration−rotation spectra obtained with an infrared interferometer shows the limits that a modern spectroscopic theory based on an empirical Hamiltonian model is able to achieve for a molecule containing a demanding large amplitude inversion motion. Apart from a limited number of perturbed transitions, the line positions and intensities are reproduced very well and there remains little room for improvement. An alternative approach using a full variational method with an exact kinetic energy operator and a potential energy surface obtained with high-quality electronic structure calculation methods such as described in ref 1 would still be some way off in accuracy compared with our present approach. Our spectral assignments will be useful in the future when the results of variational calculations are compared with experimental data.

Acknowledgment. Dr. Timo Rajamäki is thanked for experimental assistance at the early stage of this project. L.H. thanks the Academy of Finland for financial support.

Supporting Information Available: List of assigned transitions included in the fit. This material is available free of charge via the Internet at http://pubs.acs.org.

References and Notes

(1) Rajamäki, T.; Kállay, M.; Noga, J.; Valiron, P.; Halonen, L. *Mol. Phys.* **2004**, *102*, 2297.

(2) Urban, S.; D'Cunha, R.; Rao, K. N.; Papoušek, D. *Can. J. Phys.* **1984**, *62*, 1775.

(3) Špirko, V. *J. Mol. Spectrosc.* **1983**, *101*, 30.

(4) Kleiner, I.; Brown, L. R.; Tarrago, G.; Kou, Q.-L.; Picqué, N.; Guelachvili, G.; Dana, V.; Mandin, J.-Y. *J. Mol. Spectrosc.* **1999**, *193*, 46.

(5) Cottaz, C.; Kleiner, I.; Tarrago, G.; Brown, L. R.; Margolis, J. S.; Poynter, R. L.; Pickett, H. M.; Fouchet, T.; Drossart, P.; Lellouch, E. *J. Mol. Spectrosc.* **2000**, *203*, 285.

(6) Rajamäki, T.; Miani, A.; Halonen, L. *J. Chem. Phys.* **2003**, *118*, 6358.

(7) Coldwell, S. M.; Carter, S.; Handy, N. C. *Mol. Phys.* **2003**, *101*, 523.

(8) Lin, H.; Thiel, W.; Yurhenko, S.; Carvajal, M.; Jensen, P. *J. Chem. Phys.* **2002**, *117*, 11265.

(9) Leonard, C.; Carter, S.; Handy, N. *Chem. Phys. Lett.* **2003**, *370*, 360.

(10) Rajamäki, T.; Miani, A.; Halonen, L. *J. Chem. Phys.* **2003**, *118*, 10929.

(11) Saito, S.; Ozeki, H.; Ohishi, M.; Yamamoto, S. *Astrophys. J.* **2000**, *535*, 227.

(12) Shah, R. Y.; Wootten, A. *Astrophys. J.* **2001**, *554*, 933. Hatchell, J. *Astron. Astrophys.* **2003**, *403*, L25.

(13) Cohen, E. A.; Pickett, H. M. *J. Mol. Spectrosc.* **1982**, *93*, 83.

(14) Coudert, L.; Valentin, A.; Henry, L. *J. Mol. Spectrosc.* **1986**, *120*, 185.

(15) Job, V. A.; Kartha, S. B.; Kartha, V. B.; Thakur, K. B. *J. Mol. Spectrosc.* **1986**, *120*, 205.

(16) Job, V. A.; Kartha, S. B.; Singh, K.; Kartha, V. B. *J. Mol. Spectrosc.* **1987**, *126*, 290.

(17) Fusina, L.; Di Lonardo; G.; Johns, J. W. C.; Halonen, L. *J. Mol. Spectrosc.* **1988**, *127*, 240.

(18) De Lucia, F. C.; Helminger, P. *J. Mol. Spectrosc.* **1975**, *54*, 200.

(19) Kartha, S. B.; Singh, K.; Job, V. A.; Kartha, V. B. *J. Mol. Spectrosc.* **1988**, *129*, 86.

(20) Snels, M.; Hollenstein, H.; Quack, M. *J. Chem. Phys.* **2003**, *119*, 7893.

(21) Henck, S. A.; Mason, M. A.; Yan, W.-B.; Lehmann, K. K.; Coy, S. L. *J. Chem. Phys.* **1995**, *102*, 4772.; *ibid.*, 4783.

(22) Herzberg, G. *Infrared and Raman Spectra of Polyatomic Molecules*; Van Nostrand: New York, 1945.

(23) Guelachvili, G.; Birk, M.; Bordé, Ch. J.; Brault, J. W.; Brown, L. R.; Carli, B.; Cole, A. R. H.; Evenson, K. M.; Fayt, A.; Hausamann, D.; Johns, J. W. C.; Kauppinen, J.; Kou, Q.; Maki, A. G.; Rao, K. N.; Toth, R. A.; Urban, W.; Valentin, A.; Vèrges, J.; Wagner, G.; Wappelhorst, M. H.; Wells, J. S.; Winnewisser, B. P.; Winnewisser, M. *Pure Appl. Chem.* **1996**, *68*, 193. Guelachvili, G.; Rao, K. N. *Handbook of Infrared Standards*; Academic: New York, 1986.

(24) Sasada, H.; Endo, Y.; Hirota, E.; Poynter, R. L.; Margolis, J. S. *J. Mol. Spectrosc.* **1992**, *151*, 33.

(25) Watson, J. K. G. *Vibrational Spectra and Structure*; Durig, J. R., Ed.; Elsevier: Amsterdam, 1977; Vol. 6, p 1.

(26) Gordy, W.; Cook, R. L. *Microwave Molecular Spectra*; Interscience: New York, 1970.

(27) Papoušek, D.; Aliev, M. R. *Molecular Vibrational/Rotational Spectra*; Academia, Praque, 1982.

(28) Birss, F. W. *Mol. Phys.* **1976**, *31*, 491.